

## Mitochondrial Modulation of Apoptosis Induced by Low-dose Radiation in Mouse Testicular Cells\*

FANG Fang<sup>1,+</sup>, GONG Ping Sheng<sup>2,+</sup>, ZHAO Hong Guang<sup>1,3</sup>, BI Yu Jing<sup>4</sup>,  
ZHAO Gang<sup>1</sup>, GONG Shou Liang<sup>1,#</sup>, and WANG Zhi Cheng<sup>1,#</sup>

1. Key Laboratory of Radiobiology, Ministry of Health, School of Public Health, Jilin University, Changchun 130021, Jilin, China; 2. Key Laboratory for Molecular Enzymology and Engineering, Ministry of Education, Changchun 130023, Jilin, China; 3. Nuclear Medicine, First Hospital of Jilin University, Changchun 130021, Jilin, China; 4. State Key Laboratory of Pathogen and Biosecurity, Academy of Military Medical Sciences, Beijing 100071, China

### Abstract

**Objective** To investigate whether apoptosis induced by low-dose radiation (LDR) is regulated by mitochondrial pathways in testicular cells.

**Methods** Male mice were exposed to whole-body LDR, and changes in mitochondrial function and in expression of apoptotic factors were analyzed in the testicular cells as follows. Total nitric-oxide synthase (T-NOS) and Na<sup>+</sup>/K<sup>+</sup> ATPase activities were biochemically assayed. Reactive oxygen species (ROS) and mitochondrial membrane potential ( $\Delta\psi_m$ ) were determined by flow cytometry using fluorescent probes. Levels of mRNAs encoding cytochrome c (Cyt c) and apoptosis-inducing factor (AIF) were quantified by real-time reverse-transcription PCR (RT-PCR). Expression of Cyt c, AIF, caspase-9, and caspase-3 at the protein level was assessed by western blotting and immunohistochemistry.

**Results** LDR induced an increase in T-NOS activity and ROS levels, and a decrease in Na<sup>+</sup>/K<sup>+</sup> ATPase activity and mitochondrial  $\Delta\psi_m$ , in the testicular cells. The intensity of these effects increased with time after irradiation and with dose. The cells showed remarkable swelling and vacuolization of mitochondria, and displayed a time- and dose-dependent increase in the expression of Cyt c, AIF, procaspase-9, and procaspase-3. Activation of the two procaspases was confirmed by detection of the cleaved caspases. The changes in expression of the four apoptotic factors were mostly limited to spermatogonia and spermatocytes.

**Conclusion** LDR can induce testicular cell apoptosis through mitochondrial signaling pathways.

**Key words:** Mitochondria; Low-dose radiation; Testis; Apoptosis; Cytochrome c

*Biomed Environ Sci*, 2013; 26(10):820-830 doi: 10.3967/bes2013.005

ISSN: 0895-3988

[www.besjournal.com/fulltext](http://www.besjournal.com/fulltext)

CN: 11-2816/Q

Copyright ©2013 by China CDC

\*This study was supported by the National Natural Science Foundation of China (30970681) and Basic Research and Operating Expenses of Jilin University (200903116).

#Correspondence should be addressed to GONG Shou Liang, Tel: 86-431-85619443; Fax: 86-431-85619486; E-mail: gongsl@163.com; WANG Zhi Cheng, E-mail: zhicheng123a@126.com

+These authors contributed equally to this work.

Biographical note of the first author: FANG Fang, female, born in 1981, Ph. D, majoring in radiobiology and cancer gene-radiotherapy.

Received: June 5, 2012

Accepted: February 5, 2013

## INTRODUCTION

**A**poptosis, the process of programmed cell death<sup>[1]</sup>, is characterized by cellular shrinkage, condensation of chromatin and cytoplasm, and chromatin fragmentation. It plays a crucial role in controlling tissue development and homeostasis, and its dysfunction can lead to autoimmune disease or cancer<sup>[2]</sup>. Spermatogenesis is a dynamic process, involving a balance between cell survival and death, in which spermatogonia produce spermatozoa via intermediate cell types known as spermatocytes and spermatids<sup>[3]</sup>. Spermatogonia and spermatocytes undergo mitotic proliferation and meiotic division respectively, and spermatids differentiate into spermatozoa to form the germ cell population of the testes<sup>[4]</sup>. Not all spermatogonia become mature spermatozoa, because some cells spontaneously die by apoptosis at different stages of the process. In adult rats, up to 75% of the cell loss occurs during spermatogonial development. In the seminiferous tubules, apoptosis of spermatogenic cells is a normal process that contributes to testicular homeostasis by reducing the number of germ cells when they are excessive, or by removing abnormal spermatogenic cells damaged by toxins<sup>[4-6]</sup>. In addition, germ cell apoptosis can be triggered by various stimuli, including hormone deprivation, heat, radiation exposure and some endocrine disruptors such as mono-(2-ethylhexyl)phthalate<sup>[6-9]</sup>. Germ cell apoptosis induced by exposure of the testes to ionizing radiation primarily affects actively dividing spermatogonia and preleptotene spermatocytes, whereas spermatids, spermatozoa and somatic cells such as Sertoli cells and Leydig cells are less affected because of their lower radiosensitivity<sup>[10-11]</sup>.

High-dose radiation (HDR) can kill many types of cells, whereas low-dose radiation (LDR) can induce death of some cell types, such as thymocytes and splenocytes, but not others. Testes are among the most radiosensitive organs. HDR mainly induces necrotic death, whereas LDR mostly leads to apoptotic death<sup>[12]</sup>. Over the past 20 years, the biological effects of LDR, especially germ cell apoptosis and genomic damage, have been the focus of intense research<sup>[13]</sup>. Our previous studies showed that LDR can induce germ cell apoptosis in a dose- and time-dependent manner<sup>[11]</sup>. Apoptosis can be induced by intrinsic and extrinsic factors, and is regulated by several mechanisms (such as the p53, Fas/FasL and mitochondrial pathways) that are found in both somatic and germ cells. Crosstalk between the

pathways occurs at multiple levels<sup>[14-19]</sup>. The Fas/FasL pathway plays a crucial role in germ cell apoptosis<sup>[8,11,20]</sup>. Radiation-induced apoptosis of germ cells is p53-dependent and involves the Fas/FasL system<sup>[8,11]</sup>. In contrast, very little is known about the role played by the mitochondrial pathway in regulating germ cell apoptosis induced by ionizing radiation.

Germ cell apoptosis in testes can be initiated by heat stress, endocrine disruptors (such as bisphenol A) and diabetes, through a process mediated by the mitochondrial signaling pathway<sup>[6,21-22]</sup>. These triggering factors can disturb redox and energy metabolism in cells, and cause structural and functional changes in mitochondria, including mitochondrial swelling, loss of mitochondrial ridges, a decrease in mitochondrial membrane potential ( $\Delta\psi_m$ ), an increase in production of reactive oxygen species (ROS), disturbance of  $Ca^{2+}$  homeostasis and a decrease in ATPase activity. Furthermore, mitochondria can sense "death signals" and commit cells to apoptosis by releasing death factors such as cytochrome c (Cyt c) and apoptosis-inducing factor (AIF) into the cytosol. In the cytosol, Cyt c binds to apoptotic protease-activating factor 1 (Apaf-1) and to caspase-9 to form a protein complex known as the apoptosome that activates other caspases, which then cleave diverse cellular substrates<sup>[23-24]</sup>. AIF can mediate apoptosis in a caspase-independent manner by interacting with DNA or by inducing ROS production<sup>[25-26]</sup>. In addition, mitochondria are a major source of intracellular ROS, which act as second messengers during apoptosis<sup>[27]</sup>. Nitric oxide (NO), produced by nitric oxide synthase (NOS), can induce mitochondrial-dependent apoptosis, a process that becomes more frequent during aging in male germ cells of Brown-Norway rats<sup>[28-29]</sup>. Additionally, mitochondrial function is crucial for germ cells during the course of spermatogenesis. Spermatozoa containing defective mitochondria produce less ATP and generate more intense oxidative stress<sup>[30]</sup>. Therefore, the mitochondrial regulatory pathway is involved in germ cell apoptosis induced by diverse factors.

Bcl-2 and Bax are known components of the mitochondrial regulatory pathway. We have previously shown that, during LDR-induced death of male germ cells, Bcl-2 protein expression decreases and Bax protein expression increases<sup>[11]</sup>. In the present study, we aimed to investigate further whether the mitochondrial pathway was involved in LDR-induced germ cell apoptosis in testes. To this purpose, we examined changes in mitochondrial

substructure and function in testicular cells of male mice that had been exposed to whole-body LDR. Our results indicate that mitochondria can modulate LDR-induced apoptotic death in testicular cells.

## MATERIALS AND METHODS

### *Animals and Irradiation*

Healthy male Kunming mice, 7-8 weeks old and weighting  $20 \pm 2$  g, were obtained from the Jilin University Experimental Animals Center, Changchun, China. They were housed in standard lighting (12 h of light and 12 h of dark) and suitable room temperature, and allowed food and water *ad libitum*. All animal procedures were approved by the Animal Care and Use Committee of Jilin University. Mice were exposed to whole-body irradiation using X-rays generated by a Philips X-ray machine (XSS 205FZ) at 180 kV and 12 mA. The dose rate of irradiation was 12.5 mGy/min, and the filters were 0.5 mm copper and 1.0 mm aluminum. To test dose-dependent effects, the mice were irradiated with 0, 25, 50, 75, 100, or 200 mGy, and killed 12 h afterwards. To test time-dependent effects, the mice were irradiated with 75 mGy, and killed 0, 3, 6, 12, 18, or 24 h afterwards. The irradiation doses and rates were selected based on a report by the United Nations Scientific Committee on Atomic Radiation (UNSCAR, 1986) and on previous studies<sup>[11,13,31-33]</sup>. Two sides of the testes were quickly removed from the killed animals for analysis. There were 5 animals in each group, and each experiment was performed three times.

### *Biochemical Assays for Na<sup>+</sup>/K<sup>+</sup> ATPase and Total NOS (T-NOS) Activities*

Mitochondrial ATPase activity was assayed by the method described by Katz and Epstein<sup>[34]</sup>. Testis tissues were weighed with an electronic balance and then shredded with eye scissors. The tissues were suspended in balanced salt solution (at 10% w/v) in centrifuge tubes, and then homogenized using a grinding pestle followed by ultrasound. Na<sup>+</sup>/K<sup>+</sup> ATPase and T-NOS activities were measured in the testis homogenates using biochemical assay kits (Nanjing Jiancheng Bioengineering Institute, Nanjing, China) and a spectrophotometer (Beckman, USA) with 660 and 530 nm excitation wavelengths, respectively.

### *Measurement of ROS Levels and Mitochondrial $\Delta\psi_m$ by Flow Cytometry*

The testis tissues were converted into single-cell

suspensions containing  $5 \times 10^5$  cells/mL. We used 2',7'-dichlorofluorescein diacetate (DCFH-DA; Sigma, USA) for detection of intracellular ROS. DCFH-DA is deacetylated inside cells to yield reduced 2',7'-dichlorofluorescein (DCFH), which ROS can convert into oxidized 2',7'-dichlorofluorescein (DCF), a fluorescent compound. Fluorescence intensity is proportional to oxidant production<sup>[35]</sup>. Rhodamine 123 (Rh123; Sigma) was used as a fluorescent probe to detect mitochondrial  $\Delta\psi_m$ , because the probe accumulates in cells in direct proportion to the intensity of the mitochondrial  $\Delta\psi_m$ <sup>[36-37]</sup>. DCFH-DA and Rh123 were added to testicular cell suspensions to yield final concentrations of 20 and 5  $\mu\text{mol/L}$ , respectively. Then, the cells were incubated at 37 °C for 30 min in the dark, washed twice with 0.01 mol/L phosphate-buffered saline (PBS), and centrifuged at  $\times 300$  g for 5 min. ROS levels and mitochondrial  $\Delta\psi_m$  were measured by mean fluorescence intensity (MFI) of 10000 cells using a flow cytometer (Becton, Dickinson and Co., USA).

### *Observation of Subcellular Structures by Transmission Electron Microscopy*

After the mice were killed, two sides of the testes were removed quickly, washed twice with 0.01 mol/L PBS, and then fixed in 2.5% glutaraldehyde at 37 °C for 2 h. The samples were then washed five times with 0.01 mol/L PBS, fixed in 1% osmic acid for 2 h, and then dyed with uranium acetate at 4 °C overnight. They were then dehydrated in gradient alcohol, saturated in pure epoxide resin for 3 h, and embedded in Epon812 resin (Sigma). The polymerization was done at 60 °C for 48 h. Ultrathin sections of 60-90 nm thickness were collected on copper grids, double-stained with uranyl acetate and lead citrate (Sigma) and then washed three times with double-distilled water. The sections were examined using a JEM-1200EX transmission electron microscope (JEOL, Japan)<sup>[38]</sup>.

### *Real-time Reverse-transcription PCR (RT-PCR)*

The testis tissues were frozen in liquid nitrogen and then placed in 2-mL Eppendorf tubes. Total RNA of the tissues was extracted using TRIzol reagent (Invitrogen, USA) following the manufacturer's protocol, and quantified by measuring the A260/A280 ratio. Complementary DNA (cDNA) was synthesized using a high-capacity reverse transcription kit (MBI Fermentas, Canada) and 1  $\mu\text{g}$  total RNA, incubated at 42 °C for 60 min, then at 70 °C for 2 min. The following primers were used:

glyceraldehyde-3-phosphate dehydrogenase (GAPDH) forward primer 5'-AAATGGTGAAGGTCGGTGTG-3' and reverse primer 5'-TGAAGGGGTCGTTGATG G-3'; Cyt c forward primer 5'-AGTCCTGGGCACA GCAGTTG-3' and reverse primer 5'-GGCACTGAGC ACATTTCTGAACA-3'; and AIF forward primer 5'-GGTCTGAAGGCGAGTAGAGCATC-3' and reverse primer 5'-CCAATAGCTTCATAGCCGACATCA-3'. The real-time PCR reaction was performed and analyzed using an MX 3000P real-time PCR system (Stratagene, USA) following the PrimeScript RT reagent kit protocol (Takara, Japan). A two-step PCR amplification procedure was performed as following: denaturation at 95 °C for 30 s, followed by 40 cycles at 95 °C for 5 s and at 60 °C for 20 s. Relative gene expressions were calculated as the ratio of mRNA for a given gene to mRNA for GAPDH in the same cDNA sample.

### **Western Blotting Assay**

Total protein was extracted from frozen testes using ice-cold lysis buffer (10 mmol/L Tris-HCl, pH 7.4; 1 mmol/L EDTA, pH 8.0; 0.1 mol/L NaCl; 1 µg/mL aprotinin; 100 µg/mL PMSF). Protein concentration was determined using a coomassie brilliant blue protein assay (Nanjing Jiancheng Bioengineering Institute). For western blotting, 20 µg extracted protein were loaded per lane, electrophoresed on 15% SDS-PAGE, and transferred to a nitrocellulose membrane (Bio-Rad, USA) that had been blocked in PBS containing 5% non-fat dry milk. The membrane was then immersed into milk for 1 h, incubated with a primary antibody at 4 °C overnight, washed twice with TBST (Tris-buffered saline containing 0.05% Tween 20, pH 7.2) to remove unbound antibodies, and incubated with horseradish peroxidase-conjugated secondary antibody (Pierce, USA) at 37 °C for 1 h. The antigen-antibody complex was visualized using an ECL system (Santa Cruz Biotechnology, Santa Cruz, CA, USA). The primary antibodies for GAPDH, Cyt c, AIF, caspase-9 and caspase-3 (Santa Cruz Biotechnology) were diluted at an appropriate ratio (GAPDH, 1:200; Cyt c, 1:200; AIF, 1:100; caspase-9, 1:300; caspase-3, 1:300), and the secondary antibody was diluted to 1:1500.

### **Immunohistochemistry Staining**

Testes from killed mice were immediately fixed in 10% neutral formalin, stepwise dehydrated in gradient alcohol, embedded in paraffin for 24 h, and then cut into 5-µm-thick sections. The sections were

attached on poly-L-lysine-coated slides, baked for 2 h, deparaffinized twice with xylol, and incubated with different alcohol concentrations (100%, 95%, 90%, 70%, and 50%). An UltraSensitive SP kit (Maixin-Bio, Fujian, China) was used for the immunohistochemistry reaction. The sections were blocked with goat serum for 10 min at room temperature, then incubated at 4 °C overnight with antibodies against Cyt c, AIF, caspase-9 and caspase-3 (1:100 dilution each, in 1% non-immune goat serum), and then saturated with biotinylated anti-goat IgG (for Cyt c and caspase-3) and anti-rabbit IgG (for AIF and caspase-9) at 37 °C for 10 min. After being washed three times with 0.1 mol/L PBS (for 3 min each time), the sections were incubated with streptavidin-peroxidase complex for 10 min at room temperature, and then with 3,3'-diaminobenzidine (DAB) for color development, followed by counterstaining with hematoxylin. Sections acting as negative controls were incubated with PBS. Cyt c, caspase-9 and caspase-3 proteins were located in the cytoplasm, whereas AIF was located in nuclei and cytoplasm. For each protein, 50 seminiferous tubules from each section were analyzed under a microscope (Olympus, Japan), and three sections were examined for each animal. All measurements were made using a CMEAS-007 automatic image-analysis system. The results were reported as a percentage (number of positive cells in 100 seminiferous tubules).

### **Statistical Analysis**

All statistical analyses were done using SPSS, version 12.0 (SPSS Inc., Chicago, IL, USA). The results were presented as mean±SD and subjected to one-way ANOVA followed by Student's *t* test  $P < 0.05$  was considered significant.

## **RESULTS**

### ***Effect of LDR on Na<sup>+</sup>/K<sup>+</sup> ATPase Activity in Testicular Cells***

To determine the effects of LDR on mitochondrial ATP production in testicular cells, we first examined Na<sup>+</sup>/K<sup>+</sup> ATPase activity at different times after exposure to 75 mGy irradiation. As shown in Figure 1A, the Na<sup>+</sup>/K<sup>+</sup> ATPase activity had significantly decreased 3 h after exposure ( $P < 0.05$ ), reached the lowest level after 12 h, and then began to increase gradually. We also tested the effect of increasing radiation doses, and found that the Na<sup>+</sup>/K<sup>+</sup>

ATPase activity decreased with radiation doses between 25 mGy and 200 mGy (although the decrease obtained with 25 mGy was not statistically significant), reaching its lowest level with 75 mGy. These results indicate that LDR negatively affects mitochondrial  $\text{Na}^+/\text{K}^+$  ATPase activity, which would lead to reduced ATP production.

### Effects of LDR on T-NOS Activity and ROS Levels in Testicular Cells

It is known that ionizing radiation can induce ROS

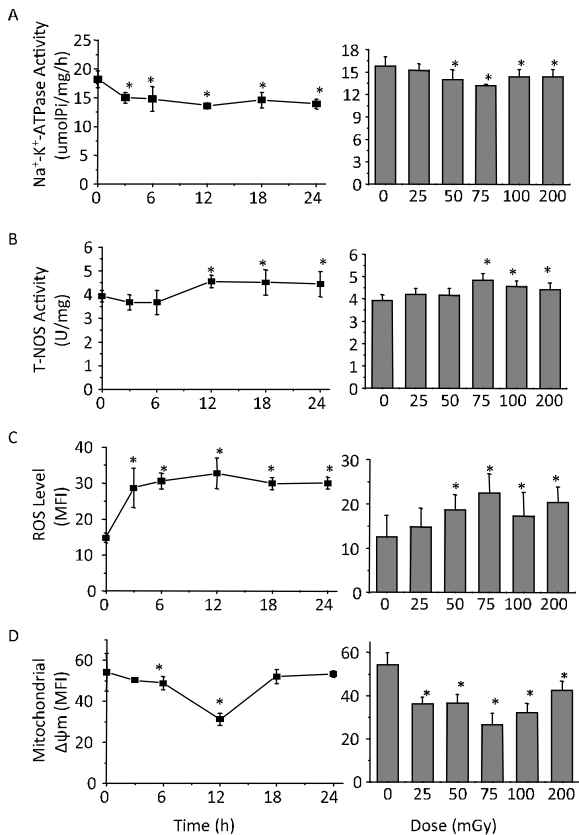


**Figure 1.** Time- and dose-dependent effects of LDR on mitochondrial function in testicular cells. Panels on the left show the effects of a 75-mGy irradiation, tested after 0, 3, 6, 12, 18, and 24 h, on  $\text{Na}^+/\text{K}^+$  ATPase activity (A), T-NOS activity (B), ROS levels (C) and mitochondrial  $\Delta\psi\text{m}$  (D). Panels on the right show the effects of different irradiation doses (0, 25, 50, 75, 100, and 200 mGy), tested after 12 h, on  $\text{Na}^+/\text{K}^+$  ATPase activity (A), T-NOS activity (B), ROS levels (C), and mitochondrial  $\Delta\psi\text{m}$  (D). The data shown are mean $\pm$ SD. \* $P$ <0.05 as compared with 0 h or with 0 mGy.

production, and that ROS and NO can trigger mitochondrial-dependent apoptosis. We measured T-NOS activity and ROS levels in the testicular cells after LDR. As shown in Figure 1B, the T-NOS activity significantly increased 12, 18, and 24 h after 75 mGy irradiation ( $P$ <0.05). It also significantly increased with 75, 100, and 200 mGy doses ( $P$ <0.05). In addition, as shown in Figure 1C, ROS levels significantly increased 3 h after 75 mGy irradiation ( $P$ <0.05), but they did not significantly increase any further afterwards during the duration of the experiment (24 h). ROS levels also increased 12 h after 25-200 mGy irradiation (the difference was significant with 50, 75, and 200 mGy;  $P$ <0.05), reaching a maximum value with 75 mGy. Therefore, LDR induces an increase in ROS levels and NOS activity in testicular cells.

### Effect of LDR on Mitochondrial $\Delta\psi\text{m}$ in Testicular Cells

A decrease in mitochondrial  $\Delta\psi\text{m}$  is considered as an early marker of apoptosis. We measured mitochondrial  $\Delta\psi\text{m}$ , expressed as MFI, in testicular cells labeled with Rh123 by flow cytometry, as previously described<sup>[36-37]</sup>. As shown in Figure 1D, mitochondrial  $\Delta\psi\text{m}$  decreased 3-12 h after 75 mGy irradiation, reaching its lowest value at 12 h; the effects at 6 and 12 h were statistically significant ( $P$ <0.05). The mitochondrial  $\Delta\psi\text{m}$  also decreased significantly 12 h after an exposure to 25-200 mGy ( $P$ <0.05), reaching the lowest value with 75 mGy. These results show that LDR reduces mitochondrial  $\Delta\psi\text{m}$  in testicular cells in a time- and dose-dependent manner.

### Effects of LDR on Mitochondrial Substructure T testicular Cells

Certain external stress signals can trigger apoptosis by inducing changes in mitochondria; mitochondria swell, their crests disappear, vacuolization of mitochondria occurs, and some mitochondrial substances are released into the cytoplasm. We studied the morphology of testicular cells by transmission electron microscope after LDR. After 75 mGy irradiation, swelling and vacuolization of mitochondria was clearly apparent in spermatogonia, spermatocytes and spermatids, whereas mitochondria retained their structural integrity in the three cell types in the absence of irradiation (Figure 2).

**Expression of Cyt c and AIF in Testicular Cells after LDR**

To investigate the roles of Cyt c and AIF in LDR-

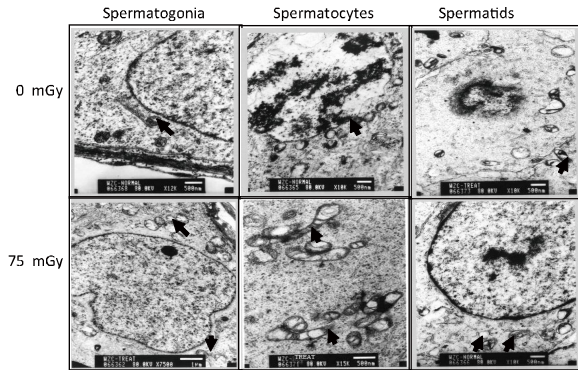


**Figure 2.** Changes in mitochondrial substructure in testicular cells after 75 mGy irradiation. Black arrows point to visible signs of mitochondrial swelling and vacuolization. Scale bars: 500 nm or 1  $\mu$ m.

induced apoptosis, we examined their expression at the mRNA level by real-time RT-PCR and at the protein level by western blotting. As shown in Figure 3A, the levels of Cyt c and AIF mRNAs in the testicular cells significantly increased at 12 h and/or 24 h after 75 mGy irradiation ( $P < 0.01$ ), reaching maximum values at 24 h. In addition, Figure 3B shows that the levels of Cyt c and AIF mRNAs significantly increased 12 h after exposure to 75 mGy (only in the case of Cyt c), 100 mGy and 200 mGy ( $P < 0.05$  or  $P < 0.01$ ), and reached the highest values with 100 mGy. Additionally, the expression of Cyt c and AIF proteins after 75 mGy irradiation increased at 12 h and decreased at 24 h (Figure 3C). The expression of both proteins increased to varying degrees 12 h after 50-200 mGy irradiation (Figure 3D). The results indicate that LDR affects Cyt c and AIF expression at the mRNA and protein levels in testicular cells in a time- and dose-dependent manner.

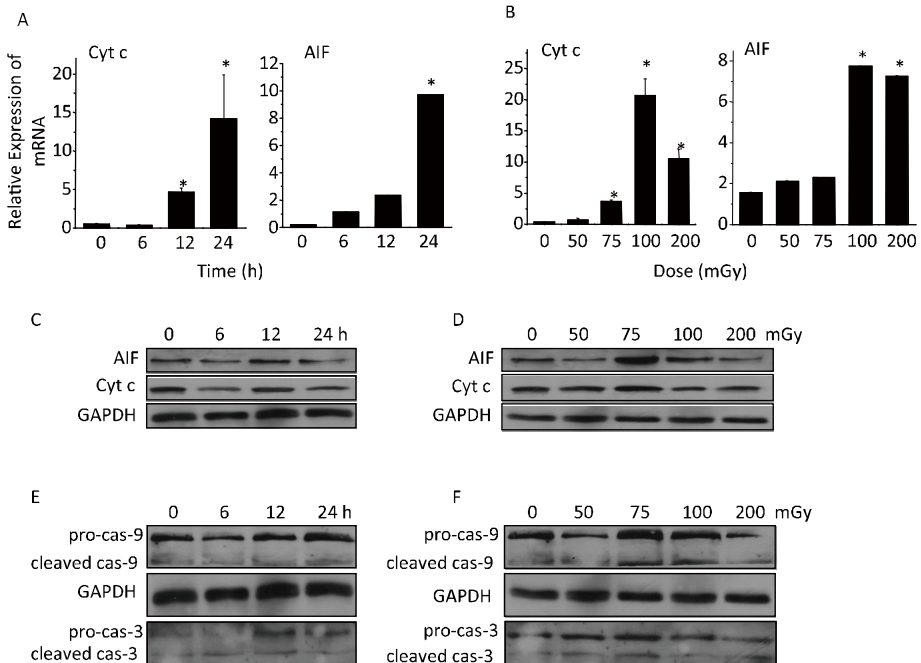


**Figure 3.** Effects of LDR on expression of Cyt c, AIF, caspase-9 and caspase-3 in testicular cells. Cyt c and AIF mRNA levels were quantified by real-time RT-PCR at various time points (0, 6, 12, and 24 h) after 75 mGy irradiation (A) and at 12 h after LDR with 0, 50, 75, 100, and 200 mGy (B). Expression of Cyt c and AIF proteins was assessed by western blotting at various time points after 75 mGy irradiation (C) and at 12 h after LDR with 0, 50, 75, 100, and 200 mGy (D). Expression of procaspase-9, procaspase-3, caspase-9, and caspase-3 proteins was analyzed by western blotting at various time points after 75 mGy irradiation (E) and at 12 h after LDR with 0, 50, 75, 100, and 200 mGy (F). Data shown are mean  $\pm$  SD. \*  $P < 0.05$ , as compared with 0 h or 0 mGy.

### Effects of LDR on the Expression and Activation of Caspase-9 and Caspase-3 in Testicular Cells

We measured the expressions of caspase-9 and caspase-3, and their uncleaved precursors, in the testicular cells by western blotting. The levels of procaspase-9 and procaspase-3 increased with time after 75 mGy irradiation, reaching maximum levels at 12 and 24 h. They also increased 12 h after LDR with 50-200 mGy, reaching the highest expression with 75 mGy. Furthermore, the levels of cleaved caspase-9 and caspase-3 also increased, following time- and dose-dependent patterns similar to those observed for the two procaspases (Figures 3E and 3F). The results indicate that LDR stimulates the expression of procaspase-9 and procaspase-3, and induces an increase in caspase-9 and caspase-3

levels, in testicular cells.

### Effect of LDR on the Expression of Cyt c, AIF, Caspase-9 and Caspase-3 in Spermatogenic Cells

We examined by immunohistochemistry the presence of Cyt c, AIF, caspase-9 and caspase-3 after LDR in the different types of spermatogenic cells. The four proteins were mainly detected in spermatogonia and spermatocytes, and less often in spermatids or spermatozoa (Figures 4 and 5). We then quantified the time- and dose-dependent effect of LDR on the presence of the four proteins in spermatogonia and spermatocytes. As shown in Figure 4, the percentage of cells expressing Cyt c or AIF increased significantly 6, 12, 18, and 24 h after 75 mGy irradiation ( $P<0.05$ ), reaching a peak at 12 h.

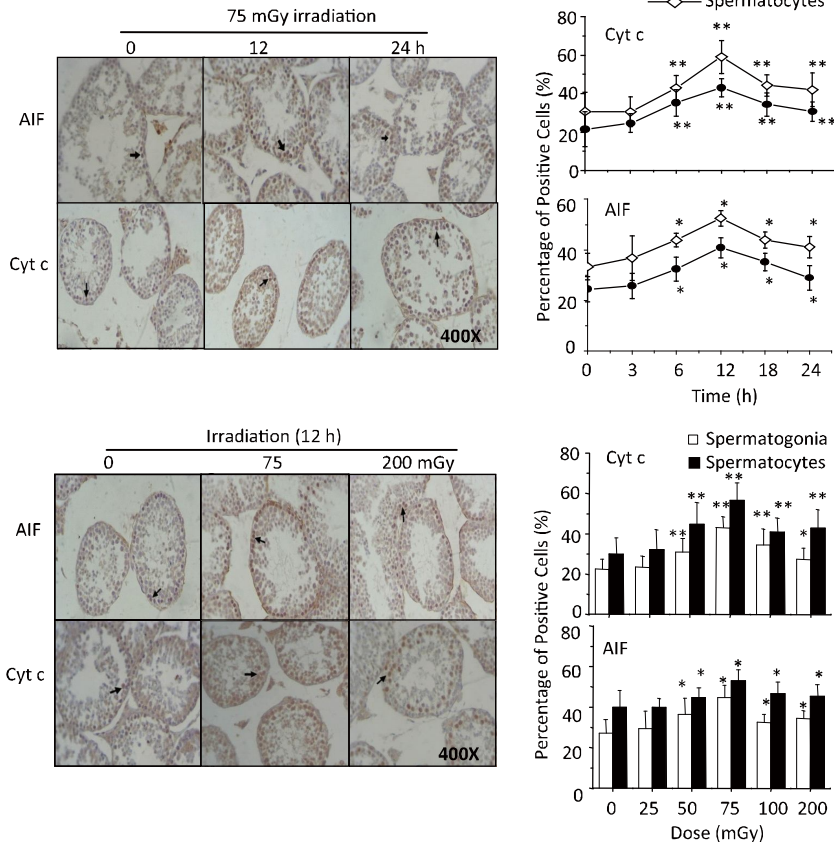


**Figure 4.** Immunohistochemical analysis of the expression of Cyt c and AIF in spermatogenic cells after LDR. Panels on the left show representative examples of cells expressing Cyt c and AIF, 0-24 h after 75 mGy irradiation (upper panel) and 12 h after 0-200 mGy irradiation (lower panel). Panels on the right show percentages of spermatogonia and spermatocytes expressing Cyt c and AIF, 0-24 h after 75 mGy irradiation (upper panel) and 12 h after 0-200 mGy irradiation (lower panel). Positive cells (i.e. expressing a given protein) in seminiferous tubules are indicated with black arrows. Magnification: 400 $\times$ . Data shown are mean $\pm$ SD. \* $P<0.05$  and \*\* $P<0.01$  as compared with 0 h or with 0 mGy.

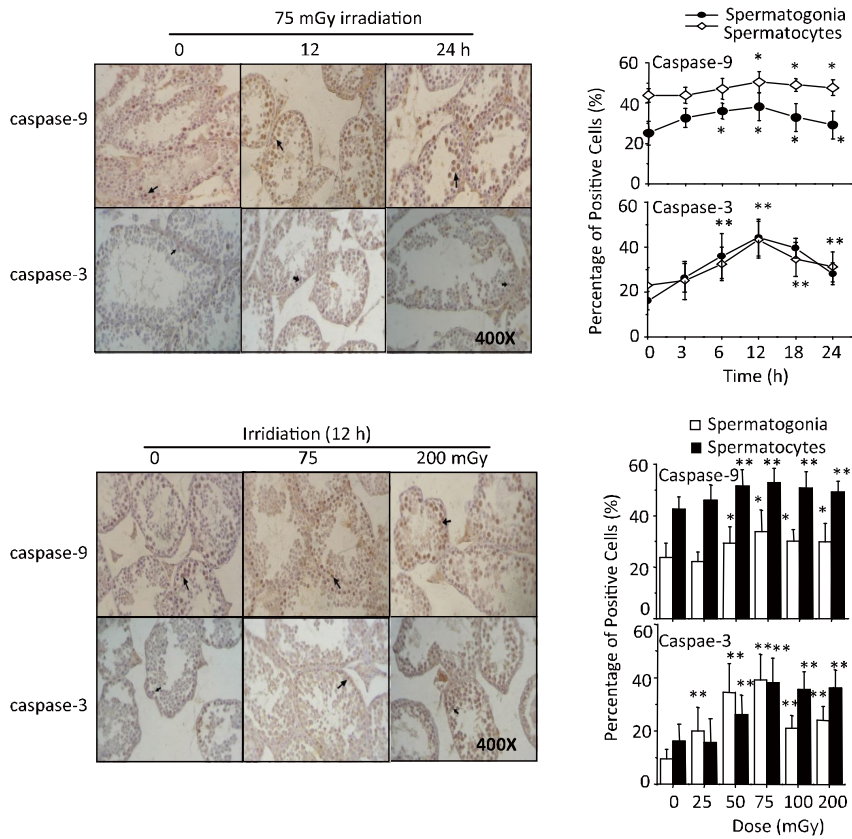


**Figure 5.** Immunohistochemical analysis of the expression of caspase-9 and caspase-3 in spermatogenic cells after LDR. Panels on the left show representative examples of cells expressing caspase-9 and caspase-3, 0-24 h after 75 mGy irradiation (upper panel) and 12 h after 0-200 mGy irradiation (lower panel). Panels on the right show percentages of spermatogonia and spermatocytes expressing caspase-9 and caspase-3, 0-24 h after 75 mGy irradiation (upper panel) and 12 h after 0-200 mGy irradiation (lower panel). Positive cells (i.e. expressing a given protein) in seminiferous tubules are indicated with black arrows. Magnification: 400x. Data shown are mean±SD. \**P*<0.05 and \*\**P*<0.01 as compared with 0 h or with 0 mGy.

They also increased 12 h after irradiation with 50, 75, 100, and 200 mGy (*P*<0.01), reaching a peak with 75 mGy. The percentage of cells expressing caspase-9- or caspase-3 also increased significantly with time and with increasing dose (*P*<0.05 and *P*<0.01), reaching peak values at 12 h and with 75 mGy, respectively. The results indicate that the effects of LDR on the expression of Cyt c, AIF, caspase-9 and caspase-3 in testicular cells are time- and dose-dependent, and are mostly limited to spermatogonia and spermatocytes.

**DISCUSSION**

Biological effects of LDR differ from those of HDR, which include hormesis and adaptive response<sup>[39-40]</sup>. The differences between LDR- and

HDR-induced effects may be attributed to differences in radiosensitivity of various cell types. Some testicular somatic cells, such as Sertoli cells and Lydig cells, are resistant to radiation; however, the testes are among the most radiosensitive organs. LDR and HDR induce death of male germ cells through different mechanisms: LDR induces apoptosis, whereas HDR induces necrosis<sup>[12]</sup>. Apoptosis plays a crucial role in eliminating excessive, genetically abnormal or damaged germ cells, thereby providing a balance between somatic and germ cell numbers<sup>[13,41]</sup>. If germ cells impaired by ionizing radiation are not eliminated, they can suffer genomic changes that can have negative effects on the next generation.

In a previous study, we demonstrated that LDR (up to 200 mGy) can induce apoptosis in mouse



germ cells through the p53 and Fas/FasL signaling pathways; in addition, a concomitant decrease in Bcl-2 expression and an increase in Bax expression suggested that a mitochondrial pathway might also regulate LDR-induced germ cell apoptosis<sup>[11,13]</sup>. In the present study, we aimed to explore in detail the mitochondrial modulation of LDR-induced apoptosis in testicular cells.

Apoptosis has a role in the loss of testicular germ cells in animals and humans, and is therefore important for male fertility<sup>[42]</sup>. Several factors such as heat, testicular toxicants and streptozotocin induce apoptosis through a mitochondrial-dependent pathway in testicular cells<sup>[6,18,22,43]</sup>. However, the apoptotic mechanisms triggered by ionizing radiation, especially LDR, are poorly understood. Mitochondria are the main source of ROS in cells, and oxidative stress and ROS are associated with apoptosis in many cell types including spermatogenic cells<sup>[44]</sup>. Indeed, certain antioxidants such as allopurinol and *N*-acetylcysteine can protect testicular germ cells from apoptosis<sup>[45-47]</sup>. Furthermore, NO acts on mitochondria to induce mitochondrial-dependent apoptosis, which increases male germ-cell death during aging in Brown-Norway rats<sup>[28-29]</sup>. Therefore, improving mitochondrial function can lead to a significant decrease in the level of oxidants in cells<sup>[48]</sup>. Several key events during cell apoptosis induced by ionizing radiation are related to mitochondria: decreased ATP production, increased ROS generation, decreased mitochondrial  $\Delta\psi_m$ , mitochondrial swelling, changes in mitochondrial inner substructure, increased mitochondrial permeability through the PTPC (permeability transition pore complex), and release of Cyt c, AIF, and caspases into the cytoplasm. All these changes are consistent with dysfunction and structural damage of mitochondria.

The results of the present study strongly suggest that LDR induces changes in the mitochondria of mouse testicular cells. We found that T-NOS activity and ROS levels increase after LDR, and that  $\text{Na}^+/\text{K}^+$  ATPase activity and mitochondrial  $\Delta\psi_m$  decrease. These changes display significant time- and dose-dependent patterns, and the effect of radiation on these parameters generally peaks at 12 h (after 75 mGy irradiation) and with 75 mGy (when different doses, up to 200 mGy, are tested). These results are consistent with apoptosis being induced by LDR in the germ cells<sup>[11]</sup>. Our finding that LDR induces increased T-NOS activity suggests that mitochondria may be damaged by NO after LDR; it is

known that NOS inhibitors such as *N*<sup>G</sup>-nitro-L-arginine methyl ester (L-NAME) can decrease NO production and reduce germ cell apoptosis<sup>[49]</sup>. In addition, our results support the notion that ROS have a role in apoptosis, although there are opposed views on this issue<sup>[50]</sup>. ROS generation in cells is expected to cause mitochondrial dysfunction<sup>[51]</sup>. Indeed, we found that mitochondrial  $\Delta\psi_m$  in the testicular cells decreases significantly after LDR, an indication of mitochondrial dysfunction. The LDR-induced decrease in  $\text{Na}^+/\text{K}^+$  ATPase activity might also lead to apoptosis by lowering intramitochondrial concentrations of  $\text{K}^+$ , which can in turn affect mitochondrial function by altering  $\Delta\psi_m$ <sup>[52]</sup>. Moreover, increased ROS generation can be not only a cause but also a consequence of mitochondrial dysfunction, leading to inhibition of  $\text{Na}^+/\text{K}^+$  ATPase activity<sup>[53-54]</sup>. In addition, we observed swelling and vacuolization of mitochondria in spermatogonia, spermatocytes and spermatids after LDR. Taken together, our results indicate that LDR can induce mitochondrial dysfunction in mouse testicular cells, and provide evidence of potential mechanisms involved in LDR-induced apoptosis.

Once mitochondrial dysfunction occurs, Cyt c and AIF are released from mitochondria into the cytoplasm. The release of Cyt c could be due to a decrease in mitochondrial  $\Delta\psi_m$  or to the presence of a specific transmembrane channel related to Bax, although this has not been confirmed<sup>[55-56]</sup>. In the cytoplasm, Cyt c interacts with Apaf-1 and caspase-9 to form the apoptosome. This results in the activation of caspase-9, which then cleaves other caspases (caspases-3, -6, and -7) that degrade many protein substrates, leading to cell death<sup>[23-24,57]</sup>. Caspase-3 also activates endonucleases that degrade cellular DNA. Additionally, AIF mediates apoptosis in a caspase-independent manner by interacting with DNA or by increasing ROS production<sup>[25-26]</sup>. On the basis of all these theories and previous findings, we decided to measure the expression of Cyt c and AIF at the mRNA and protein levels in the testicular cells after LDR, and to observe whether procaspase-9 and procaspase-3 were cleaved into active fragments. After testing several time points and radiation doses, we found that Cyt c and AIF mRNAs reach maximum levels at 24 h (after 75 mGy irradiation) and with 100 mGy (when testing up to 200 mGy doses). However, Cyt c and AIF proteins reach maximum levels at 12 h and with 75 mGy. The different effects of LDR on mRNA and protein levels for the two proteins could

be due to differences between transcription regulation and translation regulation. In addition, we observed a decrease in Cyt c protein expression 6 h after irradiation, which could be the result of Cyt c being used to form the apoptosome. Nevertheless, the effects of LDR on the expression of Cyt c and AIF are basically consistent with the time- and dose-dependent effects observed in germ-cell apoptosis and testicular-cell mitochondrial dysfunction parameters, which suggests that the changes in Cyt c and AIF expression participate in the regulation of LDR-induced apoptosis in testicular cells. In addition, we found that the levels of procaspase-9 and procaspase-3 increase in a time- and dose-dependent manner after LDR, and that both proteins are cleaved into active fragments. The expression of cleaved caspase-3 increases in a time- and dose-dependent manner, whereas that of cleaved caspase-9 follows a dose-dependent, but not a time-dependent, pattern. Therefore, our results indicate that LDR can induce the release of Cyt c and AIF proteins from mitochondria into the cytosol, and subsequently activate caspase-9 and caspase-3 in mouse testicular cells.

We have previously shown that LDR-induced apoptosis in germ cells occurs mainly in spermatogonia and spermatocytes. In the present study, we determined the presence of Cyt c, AIF, caspase-9 and caspase-3 by immunohistochemistry in testicular cells after LDR. We found that the four proteins are produced mainly in spermatogonia and spermatocytes, and that their presence follows time- and dose-dependent patterns that are similar to those observed for LDR-induced apoptosis.

In summary, the present study further underscores the importance of the mitochondrial modulation of LDR-induced apoptosis in mouse testicular cells. We demonstrate that LDR causes mitochondrial dysfunction (as indicated by changes in ROS levels, T-NOS activity, Na<sup>+</sup>-K<sup>+</sup>-ATPase activity and mitochondrial  $\Delta\psi_m$ ) and alterations in mitochondrial substructure in mouse testicular cells. Furthermore, LDR leads to increased expression of Cyt c and AIF at the mRNA and protein levels. LDR also increases the levels of caspase-9, caspase-3 and their cleaved active forms. Moreover, we show that the increase in the levels of both caspases is limited to spermatogonia and spermatocytes. These findings and our previous results<sup>[11]</sup> support the notion that mitochondrial pathways have a key role in LDR-induced apoptosis in testicular cells.

## REFERENCES

1. Kerr JF, Wyllie AH, Currie AR. Apoptosis: a basic phenomenon with wide-ranging implications in tissue kinetics. *Br J Cancer*, 1972; 26, 239-57.
2. Lorenzo HK, Susin SA. Mitochondrial effectors in caspase-independent cell death. *FEBS Lett*, 2004; 557, 14-20.
3. Lizama C, Alfaro I, Reyes JG, et al. Up-regulation of CD95 (Apo-1/Fas) is associated with spermatocyte apoptosis during the first round of spermatogenesis in the rat. *Apoptosis*, 2007; 12, 499-512.
4. Russell LD, Chiarini-Garcia H, Korsmeyer SJ, et al. Bax-dependent spermatogonia apoptosis is required for testicular development and spermatogenesis. *Biol Reprod*, 2002; 66, 950-8.
5. Print CG, Loveland KL. Germ cell suicide: new insights into apoptosis during spermatogenesis. *Bioessays*, 2000; 22, 423-30.
6. Hikim AP, Lue Y, Yamamoto CM, et al. Key apoptotic pathways for heat-induced programmed germ cell death in the testis. *Endocrinology*, 2003; 144, 3167-75.
7. Vera Y, Erkkilä K, Wang C, et al. Involvement of p38 mitogen-activated protein kinase and inducible nitric oxide synthase in apoptotic signaling of murine and human male germ cells after hormone deprivation. *Mol Endocrinol*, 2006; 20, 1597-609.
8. Embree-Ku M, Venturini D, Boekelheide K. Fas is involved in the p53-dependent apoptotic response to ionizing radiation in mouse testis. *Biol Reprod*, 2002; 66, 1456-61.
9. Lambrot R, Muczynski V, Lécureuil C, et al. Phthalates impair germ cell development in the human fetal testis *in vitro* without change in testosterone production. *Environ Health Perspect*, 2009; 117, 32-7.
10. Lee K, Park JS, Kim YJ, et al. Differential expression of Prx I and II in mouse testis and their up-regulation by radiation. *Biochem Biophys Res Commun*, 2002; 296, 337-42.
11. Liu G, Gong P, Zhao H, et al. Effect of low-level radiation on the death of male germ cells. *Radiat Res*, 2006; 165, 379-89.
12. Hamer G, Gademan IS, Kal HB, et al. Role for c-Abl and p73 in the radiation response of male germ cells. *Oncogene*, 2001; 20, 4298-304.
13. Liu G, Gong P, Bernstein LR, et al. Apoptotic cell death induced by low-dose radiation in male germ cells: hormesis and adaptation. *Crit Rev Toxicol*, 2007; 37, 587-605.
14. Bozec A, Chuzel F, Chater S, et al. The mitochondrial-dependent chronically affected in testicular germ cell death in adult in utero to anti-androgens. *J Endocrinol*, 2004; 183, 79-90.
15. Cisternas P, Moreno RD. Comparative analysis of apoptotic pathways in rat, mouse, and hamster spermatozoa. *Mol Reprod Dev*, 2006; 73, 1318-25.
16. Koji T, Hishikawa Y. Germ cell apoptosis and its molecular trigger in mouse testes. *Arch Histol Cytol*, 2003; 66, 1-16.
17. Morales E, Ferrer C, Zuasti A, et al. Apoptosis and molecular pathways in the seminiferous epithelium of aged and photoinhibited Syrian hamsters (*Mesocricetus auratus*). *J Androl*, 2007; 28, 123-35.
18. Green DR. Apoptotic pathways: paper wraps stone blunts scissors. *Cell*, 2000; 102, 1-4.
19. Hengartner MO. The biochemistry of apoptosis. *Nature*, 2000; 407, 770-6.
20. Pareek TK, Joshi AR, Sanyal A, et al. Insights into male germ cell apoptosis due to depletion of gonadotropins caused by GnRH antagonists. *Apoptosis*, 2007; 12, 1085-100.

21. Wang Q, Zhao XF, Ji YL, et al. Mitochondrial signaling pathway is also involved in bisphenol A induced germ cell apoptosis in testes. *Toxicol Lett*, 2010; 199, 129-35.
22. Amaral S, Mota PC, Lacerda B, et al. Testicular mitochondrial alterations in untreated streptozotocin-induced diabetic rats. *Mitochondrion*, 2009; 9, 41-50.
23. Katoh I, Tomimori Y, Ikawa Y, et al. Dimerization and processing of procaspase-9 by redox stress in mitochondria. *J Biol Chem*, 2004; 279, 15515-23.
24. McDonnell MA, Wang D, Khan SM, et al. Caspase-9 is activated in a cytochrome c-independent manner early during TNF $\alpha$ -induced apoptosis in murine cells. *Cell Death Diff*, 2003; 10, 1005-15.
25. Lipton SA, Bossy-Wetzel E. Dueling activities of AIF in cell death versus survival: DNA binding and redox activity. *Cell*, 2002; 111, 147-50.
26. Zhang X, Chen J, Graham SH, et al. Intracellular localization of apoptosis inducing factor(AIF) and large scale and fragmentation after traumatic brain injury in rats and in neuronal cultures exposed to peroxyxynitrite. *J NeuroChem*, 2002; 82, 181-91.
27. Varbiro G, Veres B, Gallyas F Jr, et al. Direct effect of taxol on free radical formation and mitochondrial permeability transition. *Free Radic Biol Med*, 2001; 31, 548-58.
28. Brookes PS, Salinas EP, Darley-Usmar K, et al. Concentration-dependent effects of nitric oxide on mitochondrial permeability transition and cytochrome c release. *J Biol Chem*, 2000; 275, 20474-9.
29. Hikim AP, Vera Y, Vernet D, et al. Involvement of nitric oxide-mediated intrinsic pathway signaling in age-related increase in germ cell apoptosis in male Brown-Norway rats. *J Gerontol Biol Sci*, 2005; 60, 702-8.
30. Wei YH, Kao SH. Mitochondrial DNA mutation and depletion are associated with decline of fertility and motility of human sperm. *Zoolog Stud*, 2000; 39, 1-12.
31. Cai L, Liu SZ. Induction of cytogenetic adaptive response of somatic and germ cells in vivo and in vitro by low-dose X-irradiation. *Int J Radiat Biol*, 1990; 58, 187-94.
32. Cai L, Wang P. Induction of a cytogenetic adaptive response in germ cells of irradiated mice with very low-dose rate of chronic gamma-irradiation and its biological influence on radiation-induced DNA or chromosomal damage and cell killing in their male offspring. *Mutagenesis*, 1995; 10, 95-100.
33. Li Y, Guo C, Wang Z, et al. Enhanced effects of TRAIL-endostatin-based double-gene-radiotherapy on suppressing growth, promoting apoptosis and inducing cell cycle arrest in vascular endothelial cells. *J Huazhong Univ Sci Technolog Med Sci*, 2012; 32, 167-72.
34. Katz AI, Epstein FH. The role of sodium-potassium-activated adenosine triphosphatase in the reabsorption of sodium by the kidney. *J Clin Invest*, 1967; 46, 1999-2011.
35. Zamzami N, Marchetti P, Castedo M, et al. Sequential reduction of mitochondrial transmembrane potential and generation of reactive oxygen species in early programmed cell death. *J Exp Med*, 1995; 182, 367-77.
36. Juan G, Cavazzoni M, Sáez GT, et al. A fast kinetic method for assessing mitochondrial membrane potential in isolated hepatocytes with rhodamine123 and flow cytometry. *Cytometry*, 1994; 15, 335-42.
37. Thannickal VJ, Fanburg BL. Reactive oxygen species in cell signaling. *Am J Lung Cell Mol Physiol*, 2000; 279, 1005-28.
38. Asahi J, Kamo H, Baba R, et al. Bisphenol A induces endoplasmic reticulum stress-associated apoptosis in mouse non-parenchymal hepatocytes. *Life Sci*, 2010; 87, 431-8.
39. Feinendegen LE. Evidence for beneficial low level radiation effects and radiation hormesis. *Br J Radiol*, 2005; 78, 3-7.
40. Cai L. Research of the adaptive response induced by low-dose radiation: where have we been and where should we go? *Hum Exp Toxicol*, 1999; 18, 419-25.
41. Sinha Hikim AP, Lue Y, Diaz-Romero M, et al. Deciphering the pathways of germ cell apoptosis in the testis. *J Steroid Biochem Mol Biol*, 2003; 85, 175-82.
42. Hikim AP, Vera Y, Elhag RI, et al. Mouse model of male germ cell apoptosis in response to a lack of hormonal stimulation. *Indian J Exp Biol*, 2005; 43, 1048-51.
43. Saradha B, Vaithinathan S, Mathur PP. Lindane induces testicular apoptosis in adult Wistar rats through the involvement of Fas-FasL and mitochondria-dependent pathways. *Toxicology*, 2009; 255, 131-9.
44. Kasahara E, Sato EF, Miyoshi M, et al. Role of oxidative stress in germ cell apoptosis induced by di(2-ethylhexyl)phthalate. *Biochem J*, 2002; 365, 849-56.
45. Kumagai A, Kodama H, Kumagai J, et al. Xanthine oxidase inhibitors suppress testicular germ cell apoptosis induced by experimental cryptorchidism. *Mol Hum Reprod*, 2002; 8, 118-23.
46. Rao AV, Shaha C. N-acetylcysteine prevents MAA induced male germ cell apoptosis: role of glutathione and cytochrome c. *FEBS Lett*, 2002; 527, 133-7.
47. Duarte F, Blaya R, Telöken PE, et al. The effects of N-acetylcysteine on spermatogenesis and degree of testicular germ cell apoptosis in an experimental model of varicocele in rats. *Int Urol Nephrol*, 2010; 42, 603-8.
48. Atamna H, Paler-Martínez A, Ames BN. N-t-Butyl hydroxylamine, a hydrolysis product of a-phenyl-N-t-butyl nitron, is more potent in delaying senescence in human lung fibroblasts. *J Biol Chem*, 2000; 275, 6741-8.
49. Taneli F, Vatanserver S, Ulman C, et al. Pre-ischemic administration of nitric oxide synthase inhibitors reduced germ cell apoptosis after spermatic vessel ligation in the rat testis. *Urol Int*, 2005; 75, 70-4.
50. Cai Z, Lin M, Wuchter C, et al. Apoptotic response to homoharringtonine in human wt p53 leukemic cells is independent of reactive oxygen species generation and implicates Bax translocation, mitochondrial cytochrome c release and caspase activation. *Leukemia*, 2001; 15, 567-74.
51. Ling YH, Liebes L, Zou Y, et al. Reactive oxygen species generation and mitochondrial dysfunction in the apoptotic response to Bortezomib, a novel proteasome inhibitor, in human H460 non-small cell lung cancer cells. *J Biol Chem*, 2003; 278, 33714-23.
52. Nobel CS, Aronson JK, van den Dobbelsteen DJ, et al. Inhibition of Na<sup>+</sup>/K<sup>+</sup>-ATPase may be one mechanism contributing to potassium efflux and cell shrinkage in CD95-induced apoptosis. *Apoptosis*, 2000; 5, 153-63.
53. Rodrigo R, Trujillo S, Bosco C, et al. Changes in (Na+K)-adenosine triphosphatase activity and ultrastructure of lung and kidney associated with oxidative stress induced by acute ethanol intoxication. *Chest*, 2002; 121, 589-96.
54. Orrenius S, Gogvadze V, Zhivotovsky B. Mitochondrial oxidative stress: implications for cell death. *Annu Rev Pharmacol Toxicol*, 2007; 47, 143-83.
55. Delivani P, Martin SJ. Mitochondrial membrane remodeling in apoptosis: an inside story. *Cell Death Differ*, 2006; 13, 2007-10.
56. Witt SN, Flower TR. alpha-Synuclein, oxidative stress and apoptosis from the perspective of a yeast model of Parkinson's disease. *FEMS Yeast Res*, 2006; 6, 1107-16.
57. Adrain C, Martin SJ. The mitochondrial apoptosome: a killer unleashed by the cytochrome seas. *Trends Biochem Sci*, 2001; 26, 390-7.